Autonomous Navigation, Guidance and Control of Small 4-wheel Electric Vehicle

Satoshi Suzuki

International Young Researchers Empowerment Center, Shinshu University, s-s-2208@shinshu-u.ac.jp

Abstract
In this study, we design autonomous navigation, guidance and control system for small four-wheel ground vehicle. Small and low-accuracy sensors (low-cost GPS, low-accuracy accelerometers) are only used for navigation and control of the UGV. Firstly, INS/GPS composite navigation system is designed to obtain high-accuracy position and velocity of the vehicle by using low-accuracy sensors. Secondly, velocity and heading controller for the vehicle are designed. Lastly, novel guidance method based on spline interpolation is proposed for precise guidance of the UGV. Whole systems designed in this research are validated by the simulation and experiments.

Keywords
small vehicle, motion control, composite navigation, extended Kalman filter, spline interpolation

1. INTRODUCTION
In the last decade, technology of autonomous vehicle has improved drastically, and autonomous vehicle are now used not only in research and development but also for various practical purposes. It is necessary to achieve autonomous navigation, guidance, and control of vehicles in order to reduce operator burden in practical tasks. Therefore, several researchers have focused on navigation, guidance, and control of various types of vehicles. Unmanned Aerial Vehicle (UAV) [Shim et al., 2002], Unmanned Ground Vehicle (UGV) [Wu et al., 2009], Unmanned Surface Vehicle (USV) [Moon et al., 2009], Autonomous Underwater Vehicle (AUV) [Byron et al., 2007] are example of autonomous vehicles. Moreover, several international competitions of autonomous vehicle have been held frequently. For example, DARPA Grand Challenge, Tsukuba Challenge, and Multi Autonomous Ground-robotic International Challenge (MAGIC) are the kinds of the competition.

In this study, we focus on the autonomous control of small 4-wheel unmanned ground vehicle at out of doors. It is extremely difficult to achieve autonomous control of a small vehicle, owing to the payload limitation and sensor restriction. In general, larger sensors have greater accuracy. Hence, the sensors that can be mounted on a small vehicle don't have enough accuracy for requirements specification. This tendency holds true for the GPS module used to measure the position and velocity of the vehicle. The GPS module used in conventional studies on autonomous vehicles have high accuracy and a high update rate. However, such GPS modules are too heavy to be mounted on a small UGV. Therefore, the accuracy and update rate of GPS module that we can use are quite low. Hence, it is necessary to develop a method to address these issues. In this paper, we design autonomous navigation, guidance and control system for small four-wheel ground vehicle using only small and inaccurate sensors. Firstly, INS/GPS composite navigation system is designed to obtain high-accuracy position and velocity of the vehicle by using low-accuracy sensors. Secondly, velocity and heading controller for the vehicle are designed. Lastly, novel guidance method based on spline interpolation is proposed for precise guidance of the UGV. Whole systems designed in this research are validated by the simulation and experiments.

2. EXPERIMENTAL SETUP
Experimental setup including UGV, sensors, and electric devices for control of UGV are introduced. Figure 1 shows the overview of our 4-wheel UGV. This vehicle equips one DC-motor for driving the wheels, and one servo-motor to steer the front wheels. The configuration of control device mounted on the UGV is shown in Figure 2, and main specifications of the device are listed in Table 1. In the control device, GPS is used for measuring position and velocity, In-

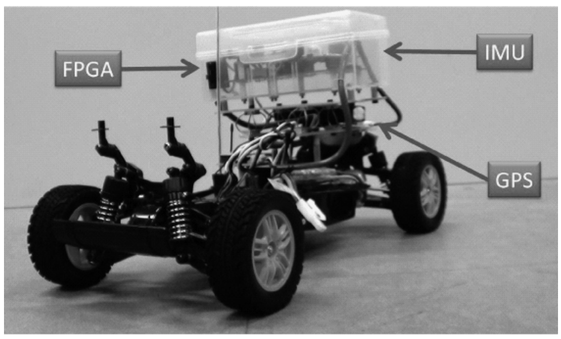

Fig. 1 Overview of small 4-wheel UGV

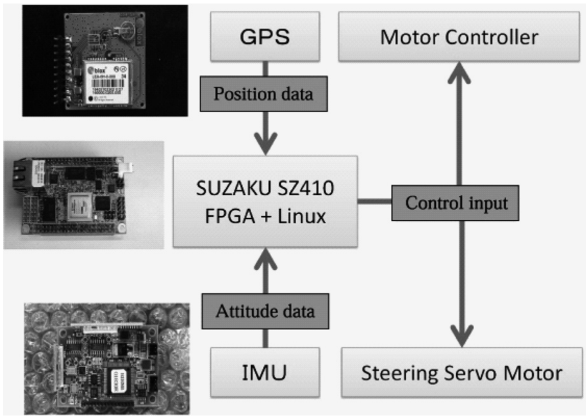

Fig. 2 Configuration of control device

Table 1 Specifications of control device

Main board (FPGA)	SUZAKU-V SZ410-U00
Wireless module	XBee-PRO
Attitude sensor	IMU-05
GPS module	u-blox 6 module
CPU core	PowerPC 405
CPU clock	350 MHz
OS	Linux (kernel 2.6)
Weight	Approximately 200 g

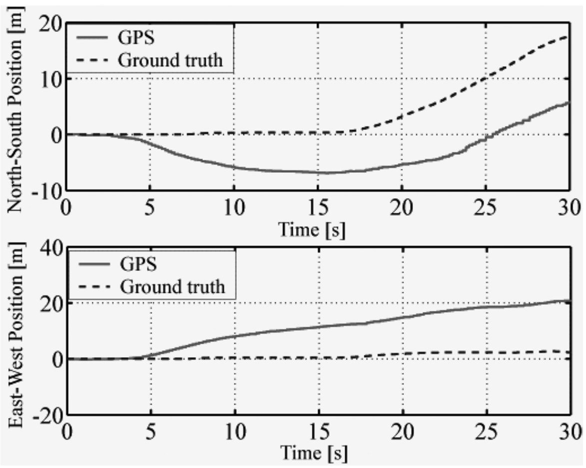

Fig. 3 Data of small GPS module

ertial Measurement Unit (IMU) is used for measuring heading angle and its rate of the UGV. We adopt only small and light weight sensors to mount them on small UGV. However, small sensors, especially for GPS, have a problem in their precision and accuracy. An example of data of small GPS module is shown in Figure 3. In this figure, solid line represents the position data measured by small GPS module, dashed line represents ground truth data obtained by RTK-GPS, the precision of which is 2 mm. Additionally, root mean square error of horizontal position on this example is 13.7 m.

From the result, it is clear that the accuracy of small GPS module is not enough for control of UGV.

3. COMPOSITE NAVIGATION SYSTEM

In order to compensate the error of small GPS module, composite navigation system is designed. The composite navigation system is constructed based on Extended Kalman Filter (EKF), which is used to integrate the inertial navigation data and small GPS data.

3.1 Coordinate system

First, we introduce the four coordinate systems used for designing the composite navigation system, and the vector notation for each coordinate system is also described. The first coordinate system is the inertial frame, and it is denoted by *I-frame*; its origin is fixed at the center of the earth. Z_i indicates the earth's polar axis; X_i and Y_i pass through points on the equator. The second coordinate system is the earth frame, and it is denoted by *E-frame*; its origin is fixed at the same point as the origin of *I-frame*. Z_e is the same as Z_i; X_e passes through a point on the equator corresponding to the 0 deg longitude at any time, and this frame rotates about Z_e in conjunction with the rotation of the earth. The third coordinate system is the navigation frame, and it is denoted by *N-frame*; its origin is fixed at the center of gravity of the UGV. X_n lies along the true north, Z_n along the direction of gravity, and Y_n along the east. In addition, the navigation algorithm is calculated in *N-frame*, and the velocity of UGV measured by GPS is expressed as vector in this frame. The last coordinate system is the body frame, and it is denoted by *B-frame*; its origin is at the same point as the origin of *N-frame*. X_b lies along the forward direction of the body, Y_b along the rightward direction, and Z_b along

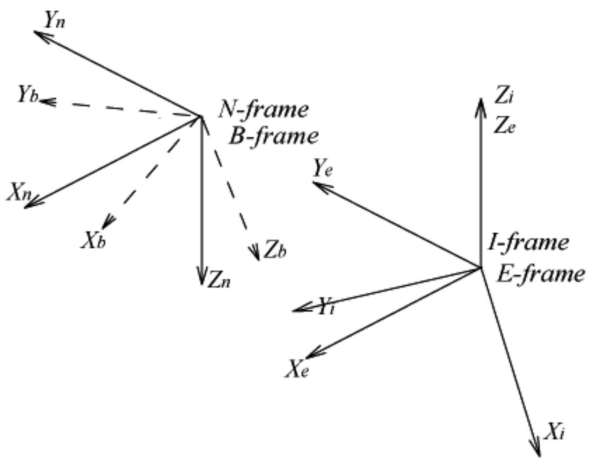

Fig. 4 Coordinate system

the downward direction. The output of an accelerometer is expressed as a vector in this frame (Figure 4). If an arbitrary vector in 3-dimensional space is denoted by r, r is expressed as r^n, and r^b, respectively in the frame defined above.

3.2 Inertial navigation

In this section, we present the derivation of the fundamental equations of inertial navigation. If V denotes the velocity vector of the UGV, the navigation equation [Rogers, 2003] is obtained as

$$\dot{V}^n = f^n - (2\omega_{ie}^n + \omega_{en}^n) \times V^n + g^n \tag{1}$$

Here, × denotes the vector product, and f^n is the acceleration vector. Now, let a^b denotes the output of accelerometers mounted on the UGV, and let $R_b^n = \left[r_1^T \; r_2^T \; r_3^T\right]^T$ denote a matrix that expresses coordinate transformation from *B-frame* to *N-frame*. Then, the relation between f^n and a^b is obtained as

$$f^n = R_b^n a^b \tag{2}$$

Here, R_b^n is a 3 × 3 matrix, and r_1, r_2, and r_3 are 1 × 3 vectors. ω_{ie}^n in (1) is a vector in *N-frame*, which expresses the angular velocity of *E-frame* relative to *I-frame*. Considering the daily rotational angular velocity of the earth as Ω_e, ω_{ie}^n is expressed as

$$\omega_{ie}^n = \left[\Omega_e \cos L \;\; 0 \;\; -\Omega_e \sin L\right]^T \tag{3}$$

Here, L denotes the latitude of the current position of the UGV. ω_{en}^n is a vector in *N-frame*, which expresses the angular velocity of *N-frame* relative to *E-frame*. Considering the longitude of the current position of the UGV as λ, ω_{en}^n is expressed as

$$\omega_{en}^n = \left[\dot{\lambda} \cos L \;\; -\dot{L} \;\; -\dot{\lambda} \sin L\right]^T \tag{4}$$

$\dot{\lambda}$ and $\dot{L}$ in (4) are quite small because the range of the operation of small UGV is sufficiently narrow and its velocity is small. Therefore, in this case, ω_{en}^n can be neglected and we did not consider ω_{en}^n in the navigation equation. Lastly, g^n is the gravitational acceleration vector, and it is simply expressed as

$$g^n = \left[0 \;\; 0 \;\; g\right]^T \tag{5}$$

Here, g represents the gravitational acceleration.

Now, considering the components of the velocity vector as $V^n = [v_n \;\; v_e \;\; v_d]^T$, and assuming that the vertical velocity of the UGV is zero, horizontal components of the inertial navigation equation are written as follows:

$$\dot{v}_n = r_1 a^b - 2 v_e \Omega_e \sin L \tag{6}$$

$$\dot{v}_e = r_2 a^b + 2 v_n \Omega_e \sin L \tag{7}$$

On the other hand, the semi-major axis and eccentricity of the earth are denoted as R_l and e, respectively, the north-south directional radius of curvature R_n and the east-west directional radius of curvature R_e of the earth are expressed as follows:

$$R_n = \frac{R_l(1-e^2)}{(1-e^2 \sin^2 L)^{\frac{3}{2}}} \tag{8}$$

$$R_e = \frac{R_l}{(1-e^2 \sin^2 L)^{\frac{1}{2}}} \tag{9}$$

Using R_n and R_e, The time derivatives of latitude L and longitude λ are obtained as follows:

$$\dot{L} = v_n / R_n \tag{10}$$

$$\dot{\lambda} = v_e / (R_e \cos L) \tag{11}$$

Equations (6), (7), (10), and (11) are the fundamental equations of the inertial navigation.

3.3 Design of composite navigation system

We describe the design of the composite navigation system using EKF. Block diagram of entire system is shown in Figure 5. The errors of small GPS module and inertial navigation are mutually compensated by using EKF. For designing EKF, process model, which expresses the dynamics of the system, are required. Hence, at first, we derive the process model. The process model is derived on the basis of equations (6), (7), (10), and (11). a^b in (6) and (7) can be obtained using the small accelerometers mounted on the UGV. However, output of small low-cost accelerometers includes a large bias error resulting in the divergence of navigation computation. Therefore in this case, we assume

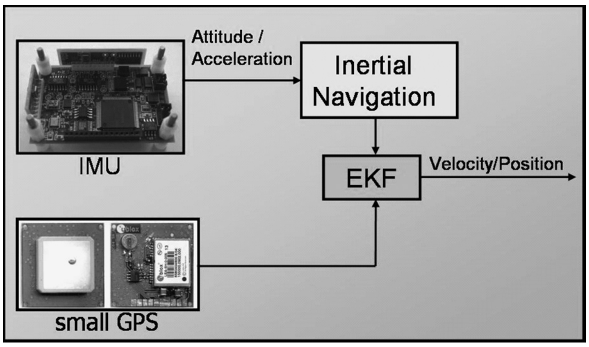

Fig. 5 Composite navigation system

that the bias error of the accelerometer has the following dynamics; we introduce it into the process model, and finally compensate it.

$$\dot{b}_{ax} = w_x,\ \dot{b}_{ay} = w_y,\ \dot{b}_{az} = w_z \tag{12}$$

Here, w_x, w_y, and w_z denote white noise. Introducing the vector $b_a = [b_{ax}\ \ b_{ay}\ \ b_{az}]^T$, (6) and (7) could be rewritten as follows:

$$\dot{v}_n = r_1(a^b - b_a) - 2v_e\Omega_e \sin L \tag{13}$$

$$\dot{v}_e = r_2(a^b - b_a) + 2v_n\Omega_e \sin L \tag{14}$$

Integrating (10)-(14), we obtain the nonlinear state-space equation as follows:

$$\begin{aligned} \dot{x} &= f(x) + Gw \\ x &= \begin{bmatrix} L & \lambda & v_n & v_e & b_{ax} & b_{ay} & b_{az} \end{bmatrix}^T \\ G &= \begin{bmatrix} 0_{3\times4} & I_{3\times3} \end{bmatrix}^T,\ w = \begin{bmatrix} w_x & w_y & w_z \end{bmatrix}^T \end{aligned} \tag{15}$$

Digitizing the above equation, the discrete-time state-space equation can be obtained. Next, the measurement equation is derived. The outputs of the system are the latitude, longitude, and horizontal velocity, obtained using small GPS module. Now, we consider the output vector of the system as $y = [L\ \ \lambda\ \ v_n\ \ v_e]^T$ then the measurement equation could be obtained as

$$\begin{aligned} y &= Hx + v \\ H &= \begin{bmatrix} I_{4\times4} & 0_{4\times3} \end{bmatrix} \end{aligned} \tag{16}$$

Here, v is a vector that expresses the measurement noise. The composite navigation system can be realized by applying the EKF algorithm to the process model represented by (15) and (16). The error of inertial navigation could be compensated by using estimated bias error of the accelerometer in (13) and (14). On the other hand, the error of position of small GPS module could be compensated by the position and velocity data of inertial navigation. As a result, the errors of small GPS module and inertial navigation are mutually compensated.

In order to verify the composite navigation system, validation experiment was carried out. In the experiment, whole devices including the GPS module were mounted on the cart which is moved manually, and RTK-GPS was also mounted to obtain ground truth data. The navigation algorithm was calculated by using the computer embedded in the FPGA board. Figure 6 shows position data and Figure 7 shows velocity data in the experiment. In these figures, solid line represents the position and velocity data estimated by composite navigation system. From Figure 6, it is shown that the position was precisely estimated by the navigation system, even though the GPS data had a huge bias error in each axis. In addition, Figure 7 shows that the velocity was also estimated precisely. Moreover, root mean square errors of the position data is less than 1.0 m, and errors of the velocity data is less than 0.25 m/s. From the results, it can be concluded that the composite navigation system was able to estimate accurate position and velocity, even though small GPS module had a large error.

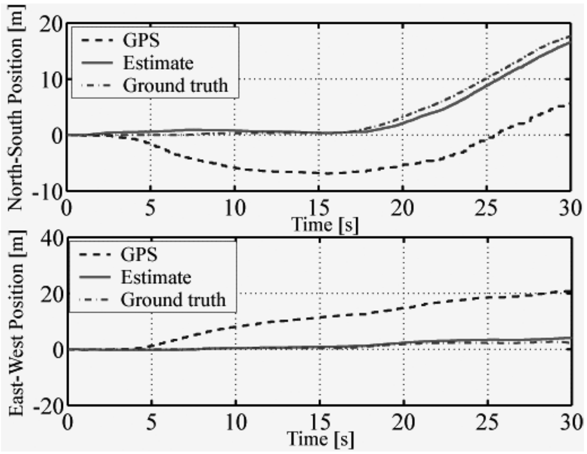

Fig. 6 Result of composite navigation (position)

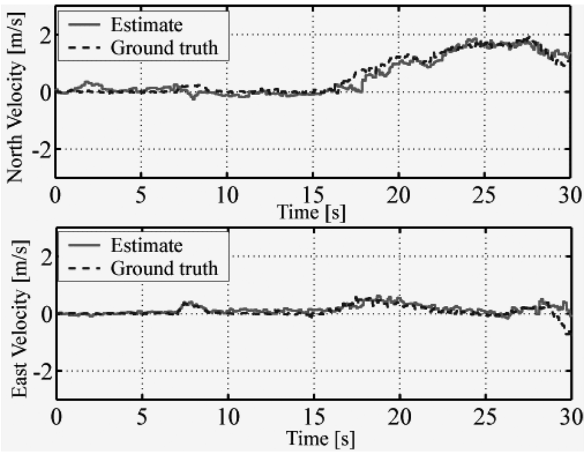

Fig. 7 Result of composite navigation (velocity)

4. CONTROL SYTEM DESIGN

In this section, velocity and heading control system of small 4-wheel vehicle are designed. Guidance of the vehicle could be achieved by realizing appropriate velocity and heading angle of the vehicle. Therefore, it is necessary for realizing the guidance of the vehicle to make the velocity and heading angle follow desired value. In the following, derivation of mathematical model of the vehicle, and control system design by using derived model are shown. First, heading angle model is derived. Assuming the forces impressed on front wheel and rear wheel are equal, the model of

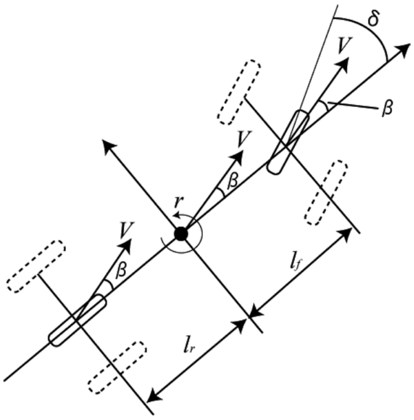

Fig. 8 2-wheel model

4-wheel vehicle become equivalent to 2-wheel model shown in Figure 8 [Abe, 2008]. In this figure, V denote the velocity of the vehicle, r: heading angular velocity, β: the slip angle of the vehicle, l_f and l_r: distance between the center of the rotation of the vehicle and each wheel, and δ is steering angle of front wheel. Now, considering mass of the vehicles as M, inertia moment of heading direction as J, and assuming that the slip angle β is sufficiently small, the dynamics of the slip angle and the heading angular velocity could be represented as

$$MV\dot{\beta} + 2(K_f + K_r)\,\beta + \{MV + \frac{2}{V}(l_f K_f - l_r K_r)\}r = 2K_f\delta \tag{17}$$

$$J\dot{r} + 2(l_f K_f - l_r K_r)\beta + \frac{2(l_f^2 K_f + l_r^2 K_r)}{V} r = 2l_f K_f \delta \tag{18}$$

Here, K_f and K_r represent cornering power of front wheel and rear wheel respectively. In this case, we consider K_f and K_r as constant. Now, considering heading angle as ψ and the state of heading dynamics as $x_h = [\psi \;\; r \;\; \beta]^T$, following state space equation could be obtained.

$$\dot{x}_h = \begin{bmatrix} 0 & 1 & 0 \\ 0 & -\dfrac{2(l_f^2 K_f + l_r^2 K_r)}{JV} & -\dfrac{2(l_f K_f - l_r K_r)}{J} \\ 0 & -1 - \dfrac{2(l_f K_f - l_r K_r)}{MV^2} & -\dfrac{2(K_f + K_r)}{MV} \end{bmatrix} x_h + \begin{bmatrix} 0 \\ \dfrac{2l_f K_f}{J} \\ \dfrac{2K_f}{JV} \end{bmatrix} \delta \tag{19}$$

Next, velocity model is derived. The velocity of the vehicle is determined by the angular velocity of the wheels driven by DC-motor. Therefore assuming the slip of the wheels is sufficiently small, the dynamics of the velocity is equivalent to the dynamics of the DC-motor. Generally, the dynamics of the DC-motor could be approximated as second order system. Thus, the dynamics of the velocity of the vehicle also could be approximated as second order transfer function shown as follows:

$$G_v(s) = \frac{b_0 s + b_1}{a_0 s^2 + a_1 s + 1} \tag{20}$$

Model parameters in (19) and (20) were determined by measurement of the physical parameters of the vehicle and comparison between simulation and experimental data. Value of the model parameters are listed in Table 2. Finally, velocity and heading controller was designed by using PID control method. P gain, I gain, and D gain of the controller was determined by

Table 2 Model parameters

Parameter	Value	Parameter	Value
M	1.82 kg	J	0.03 kgm^2
lf	0.09 m	l_r	0.21 m
K_f	0.17	K_r	0.75
a_0	0.1	a_1	1.4
b_0	0.008	b_1	0.013

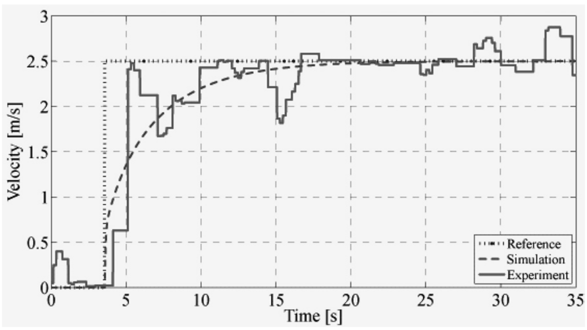

Fig. 9 Result of velocity control

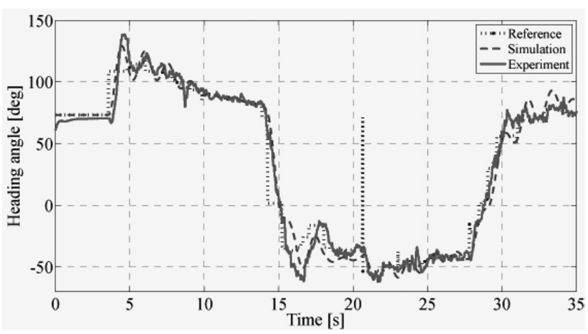

Fig. 10 Result of heading control

the simulation using derived model. In the case of velocity controller, P gain is 60, I gain is 30, and D gain is 0. On the other hand, P gain is 12, I gain is 0, and D gain is 4. Moreover, control experiment was carried out by using the controller. Results of the experiment are shown in Figure 9 and Figure 10. In the experiment, velocity reference was constant, and heading angle reference was impressed as arbitrary time varying signal. From the figures, velocity and heading angle of the vehicle could precisely follow the reference value. Hence, it is clear that the controllers designed in this section are effective for the control of the small UGV. Moreover, in these figures, simulation result accords with the experimental data. Therefore, it can be said that the validity of derived model was also shown.

5. GUIDANCE

In this section, guidance system for the UGV is designed. Most popular guidance method for vehicle is waypoint navigation method (WPN). WPN is used for the guidance of various aerial, ground, and surface vehicles. However, WPN has potentially a problem which causes destabilization of the vehicle. In order to avoid the problem, we propose novel path generation method using spline interpolation.

5.1 Waypoint navigation

WPN is a guidance method which guides the vehicle toward the goal while sequentially passing a pass point named waypoint (WP) which was set beforehand. In the case of small UGV, WPN could be achieved by controlling the heading angle of the vehicle. Figure 11 shows basic idea of WPN. In this figure, angle θ can be calculated by using current position of the vehicle, position of WP, and the heading angle of the vehicle. If the heading angle was controlled to make the angle θ become to zero, the vehicle runs towards WP and can pass WP. In other words, WPN could be achieved by setting the heading angle reference ψ_d as follows:

$$\psi_d = \begin{cases} \tan^{-1}\left(\dfrac{x_{wp}-x_v}{y_{wp}-y_v}\right) & (y_{wp} > y_v) \\ \pi - \tan^{-1}\left(\dfrac{x_{wp}-x_v}{y_{wp}-y_v}\right) & (y_{wp} < y_v,\ x_{wp} > x_v) \\ \tan^{-1}\left(\dfrac{x_{wp}-x_v}{y_{wp}-y_v}\right) - \pi & (y_{wp} < y_v,\ x_{wp} < x_v) \end{cases} \quad (21)$$

However using only (21), the attitude (heading angle) of the vehicle cannot be considered when the vehicle pass WP and go toward next WP. As a result, undesirable behavior such as hard turn and reverse run may occur at the time of a change of WP. These undesirable behaviors may cause destabilization for the vehicle in the worst case scenario. In order to avoid the problem, we propose a path generation method using spline interpolation in next section.

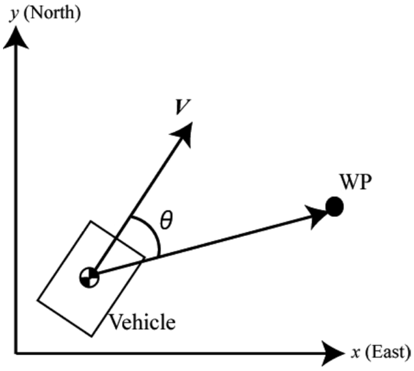

Fig. 11 Waypoint navigation

5.2 Path generation using spline interpolation

Spline interpolation is one of method for interpolating multiple given points using smooth curve. Generally in the case of spline interpolation, N points could be interpolated by using (N-1)th polynomial named spline function. However, there is a problem that computational complexity increases very much, as a number of points to interpolate increases. Therefore, in this case we divide interpolation points, and interpolate by using third spline function. Now, third spline function $S_j(x)$ for N + 1 points (x_j, y_j: $_{j} = 1 - _{N}$) is defined as

$$S_j(x) = a_j(x-x_j)^3 + b_j(x-x_j)^2 + c_j(x-x_j) + d_j \quad (22)$$

Here, suffix j means that $S_j(x)$ is a curve between j th and (j + 1) th points (Figure 12). Additionally, coefficients in (22) could be obtained as follows:

$$a_j = \frac{u_{j+1} - u_j}{6(x_{j+1} - x_j)} \quad (23)$$

$$b_j = \frac{u_j}{2} \quad (24)$$

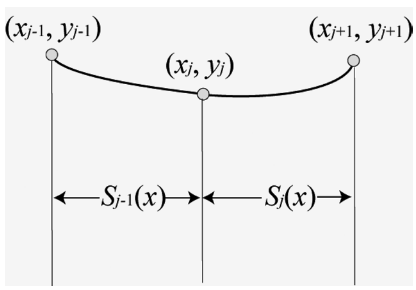

Fig. 12 Spline function

$$c_j = \frac{y_{j+1} - y_j}{x_{j+1} - x_j} - \frac{1}{6}(x_{j+1} - x_j)(2u_j + u_{j+1}) \tag{25}$$

$$d_j = y_j \tag{26}$$

Here, $u_0 = u_N = 0$, and $U = [u_1 \;\; u_2 \;\; \ldots \; u_{N\text{-}1}]^T$ is a solution of simultaneous equation defined as follows:

$$HU = V \tag{27}$$

Here, matrices in (32) are defined as

$$H = \begin{bmatrix} 2(h_0 + h_1) & h_1 & & 0 \\ h_1 & 2(h_1 + h_2) & h_2 & \\ & 0 & \ddots & \\ & & h_{N-2} & 2(h_{N-2} + h_{N-1}) \end{bmatrix}$$
$$V = [v_1 \;\; v_2 \;\; \cdots \;\; v_{N-1}]^T$$
$$h_i = x_{i+1} - x_i$$
$$v_i = 6\left[\frac{y_{i+1} - y_i}{h_i} - \frac{y_i - y_{i-1}}{h_{i-1}}\right] \tag{28}$$

In this case, traveling path of the UGV was successively generated by using three WP, previous WP, current WP, and next WP.

Finally, simulation and experiment were carried out to verify proposed path generation method. Figure 13 shows the result of the simulation. In this simulation, velocity reference was impressed as constant 2.0 m/s, and heading reference was calculated by using (21). In this figure, dashed line represents the result of conventional waypoint navigation using only (21), solid line represents the result of proposed method using (21) and path generation method by spline interpolation. Trajectory of conventional and proposed method are almost same until second WP. However, after second WP, trajectories are completely different. In particular, the trajectory of the conventional method is vibrated after third WP because the vehicle suddenly turns in this point. Moreover, in the case of conventional method, the vehicle cannot pass over third and forth WP. By contrast, hard turn is not occur and the vehicle can precisely pass over third and forth WP in the case of proposed method. Additionally, experimental result using proposed method is shown in Figure 14. In the figure, dashed line represents the traveling path generated by using proposed method. Solid line represents the trajectory of the vehicle. It is clear that the vehicle can precisely follow the traveling path. From the results, effectiveness of proposed path generation method for the guidance of the UGV is shown.

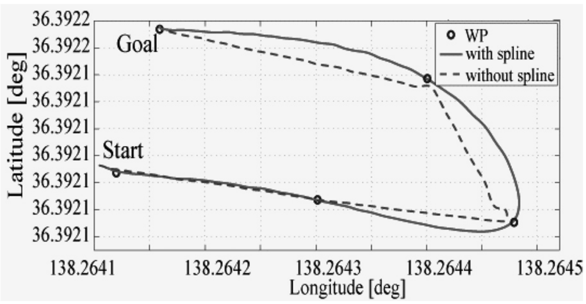

Fig. 13 Simulation result

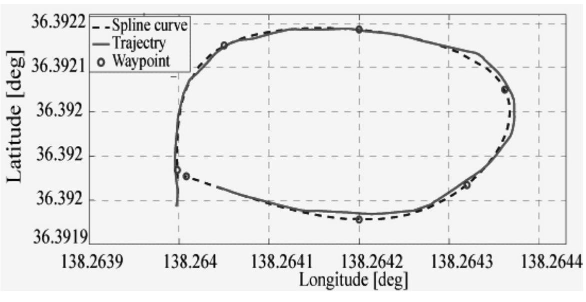

Fig. 14 Experimental result

6. CONCLSION

In this paper, we designed autonomous navigation, guidance and control system for small four-wheel ground vehicle. INS/GPS composite navigation system was designed to obtain high-accuracy position and velocity data of the UGV. Accurate estimation of position and velocity has been achieved. Vehicle motion control system including velocity and heading controller were designed. Finally, novel guidance system for the UGV based on spline interpolation was proposed for precise guidance. Whole systems designed in this research are validated by the simulation and experiments, and effectiveness of the system was shown.

References

Shim, D. H., J. Kim, and S. Sastry, A flight control system for aerial robots: Algorithm and experiments, *Control Engineering Practice*, Vol. 11, Issue.12, 1389-1400, 2003.

Wu, G., H. Sun, J. Zou, and L. Wan, Development of unmanned ground vehicles available of urban drive, *Proceedings of International Conference on Mechatronics and Automation 2009*, 611-616, 2009.

Moon, H., J. Lee, J. Kim, and D. Lee, The basic motion control strategy for the water-jet-propelled USV, *Proceedings of IEEE/ASME International Conference on Advanced Intelligent Mechatronics 2009*, 786-790, 2009.

Byron, J., and R. Tyce, Designing a vertical/horizontal AUV for deep ocean sampling, *Proceedings of OCEANS 2007*, 1-10, 2007.

Rogers, R. M., *Applied Mathematics in Integrated Navigation System Second Edition*, AIAA Educa-

tion Series, 2003.
Abe, M., *Automotive Vehicle Dynamics Theory and Applications*, Tokyo Denki University Press, 2008.

(Received April 9, 2012; accepted May 7, 2012)